Gas-Solid Fluidized Systems: Average Mass Transfer Potentials of Shallow Beds

An experimental investigation has been conducted on the direct establishment of mass transfer driving forces for the vaporization of *n*-decane from Celite particles fluidized by air. Ranges of particle sizes and reactor diameters were employed.

Concentration profiles of *n*-decane were determined and were integrated to obtain the actual average concentration difference for the entire bed. The ratio of the actual driving force to the corresponding log-mean value has been correlated with the average particle size, the fluidized bed height, and the modified Reynolds number to produce two relationships capable of predicting these ratios to within 2.5% (83 runs). The results for these mass transfer studies should also be applicable to comparable studies on heat transfer in fluidized beds.

POONG YOON
and
GEORGE THODOS

Department of Chemical Engineering
Northwestern University
Evanston, Illinois 60201

SCOPE

An issue arising from considerations of mass transfer operations in fluidized beds is the selection of the proper driving force for the calculation of the actual mass transfer coefficients. For packed beds the application of the log-mean driving force has been justified on both theoretical and experimental grounds for flow conditions of $N_{Re} > 100$. This type of driving force can be used up to the minimum fluidization state at which the individual particles of a bed assume a state of disengagement. For fluidized beds, it has been pointed out that most of the transfer occurs in the region near the bed entrance (Zabrodsky, 1963).

The complex nature of fluidized bed systems does not permit a rigorous theoretical definition of the proper driving force. However, attempts to utilize the log-mean driving force in such systems have been reported in the literature. For the mass transfer of naphthalene in fluidized beds, Chu, Kalil, and Wetteroth (1953) utilized the log-mean driving force to establish mass transfer coefficients. A log-mean driving force was also used by Sen Gupta and Thodos (1962) to develop from literature data a generalized correlation for mass and heat transfer factors for packed and fluidized beds. However, the question concerning the proper driving force remained sufficiently ambiguous and prompted Wilkins and Thodos (1969) to determine experimentally the actual concentration profile of *n*-decane within a fluidized bed of Celite particles saturated with this hydrocarbon.

This work has been continued in the present study to establish more accurate concentration profiles for a wider range of conditions than those previously investigated.

CONCLUSIONS AND SIGNIFICANCE

In this study, the following relationship has been developed from experimental data for mass transfer of *n*-decane into air for fluidized beds of Celite particles:

$$1 - f = 0.22 \frac{\left(\dfrac{h_f}{d_p} \right)^{1.5}}{\left[\dfrac{d_p G}{\mu(1 - \epsilon_f)} \right]^{0.70}}$$

where f is the ratio of the actual average concentration difference over the entire bed to the corresponding log-mean value, h_f the height of the fluidized bed, d_p the diameter of the particles, G the superficial mass velocity of the gas stream, μ the viscosity of the gas, and ϵ_f the void fraction of the fluidized bed. This relationship reproduces the experimental values of f with very good accuracy except for runs conducted with small particles in a reactor of a small diameter. For the latter case a separate relationship has been determined.

The results of this study permit the establishment of mass transfer driving forces from the parameters of the system for conditions comparable to those investigated in this study. These results should also be applicable for heat transfer in fluidized beds under similar conditions.

EXPERIMENTAL EQUIPMENT AND PROCEDURE

The experimental equipment utilized in this investigation is essentially the same employed by Wilkins and Thodos (1969). A schematic diagram of the experimental apparatus is presented in Figure 1. Celite particles of average diameters 0.309, 0.260, 0.218, and 0.183 cm were soaked in *n*-decane and then were fluidized with air. The average densities of the particles were found to range from 0.958 to 1.125 g/cm^3. The temperature was measured with fine copper-constantan thermocouples imbedded near the surface of two Celite particles. One of these particles was located inside the fluidized bed and the other above the fluidized section. Both thermocouples were attached to vertical traveling probes. During the course of a run, both

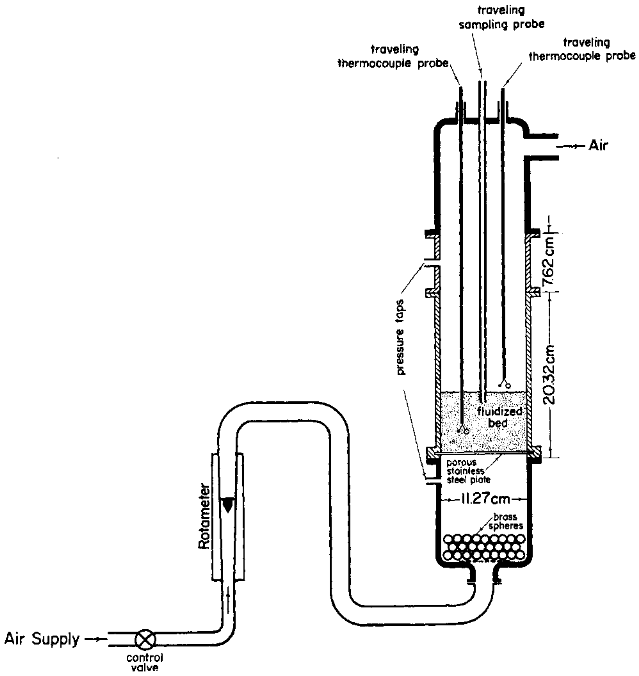

Fig. 1. Schematic diagram of experimental unit for fluidized bed studies.

thermocouples produced identical readings indicating a constant rate of drying. A stainless steel porous plate supported the fluidized bed. The flow of air before the calming section of the bed was measured with a rotameter. Approximately 1 to 1½ minutes were required to reach steady state conditions while an experimental run lasted 3 to 5 minutes. Three interchangeable reactors with inner diameters of 11.28 cm (Reactor 1), 7.47 cm (Reactor 2) and 4.44 cm (Reactor 3) were utilized.

In the course of a run, pressure drops and temperatures were measured. A traveling sampling probe (3-mm stainless steel tubing) connected to a vacuum pump was used to continuously withdraw gas samples from several locations within and above the fluidized bed. A fine stainless steel screen at the tip of this probe prevented the withdrawal of fluidized particles. By the use of an automatic sampling valve, the gas from the probe was introduced into a hydrocarbon analyzer of a flame ionization type (Beckman, Model 109A) which used nitrogen as the carrier gas. It was found necessary to heat all of the sampling lines leading to the analyzer with heating tape. The signal from the analyzer was transmitted to a recorder and the resulting response curves were integrated to obtain the hydrocarbon content of the air samples. These results permitted the establishment of the concentration profile of *n*-decane in the air for each run.

Altogether, 83 runs were completed using all four particle sizes and the three different reactors. The experimental data are summarized in Tables 1, 2, and 3.[*]

ANALYSIS OF EXPERIMENTAL DATA

Typical concentration profiles are presented in Figures 2 and 3 for two different flow rates for a particle size $d_p = 0.260$ cm and a packed bed height of 1.75 cm. Both runs were conducted in Reactor 2 ($D = 7.47$ cm). For the lower mass velocity (Run LF40-1A), the concentration profile of *n*-decane in air approaches that for packed bed conditions, while the behavior is substantially different for the higher flow rate as shown in Figure 3. The shapes of these profiles are typical for all runs of this study and are characterized by a monotonically increasing dependence on bed height. Such profiles are different from those found in the preliminary studies of Wilkins and Thodos (1969) who obtained lower concentrations of *n*-decane at the inlet of the bed and attributed this behavior to entrance effects. These different results may be attributed to the adsorption of *n*-decane vapor in the sampling line for the study of Wilkins and Thodos (1969) and to the fact that in their work the runs extended up to 10 minutes for which the rate of drying may not have remained constant.

The actual driving force for each run was established by graphical integration of the difference between the *n*-decane concentration of the air in the fluidized bed at a particular height and the saturation condition at the surface of the particles. The saturation condition was established from the readings of the two probe thermocouples and the vapor pressure relationship of *n*-decane

$$\log_{10}p = 27.561 - \frac{3443.5}{T} - 6.4066\log_{10}T \qquad (1)$$

where p is in mm of mercury and T in degrees Kelvin. A log-mean driving force $(\Delta y)_l = [(\Delta y)_i - (\Delta y)_o]/\ln[(\Delta y)_i/(\Delta y)_o]$, was calculated for each run using the inlet and outlet concentration differences for comparison with actual driving force. The actual and log-mean driving forces of each run are included in Tables 1, 2, and 3.

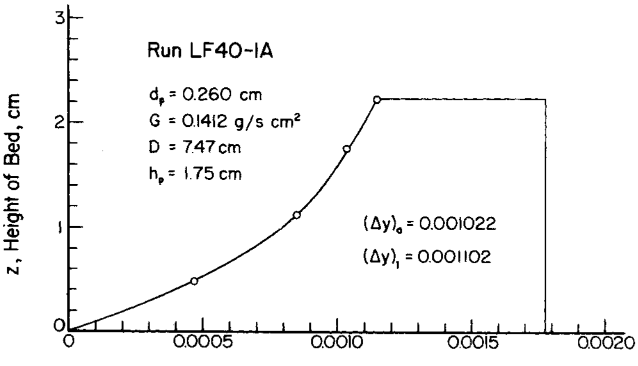

Fig. 2. Typical concentration profile for a fluidized bed of relatively low mass velocity.

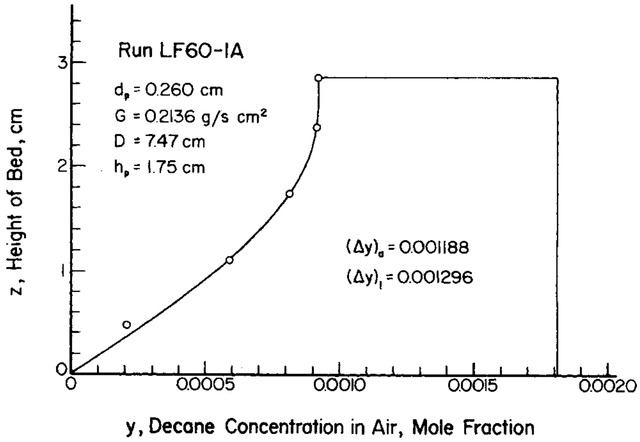

Fig. 3. Typical concentration profile for a fluidized bed of relatively high mass velocity.

The log-mean driving force represents the maximum possible average concentration difference. The actual and

---

Tables 1, 2, and 3 have been deposited as Document No. 02092 with the National Auxiliary Publications Service (NAPS), c/o Microfiche Publications, 305 East 46 Street, N. Y. 10017 and may be obtained for $1.50 for microfiche or $5.00 for photocopies.

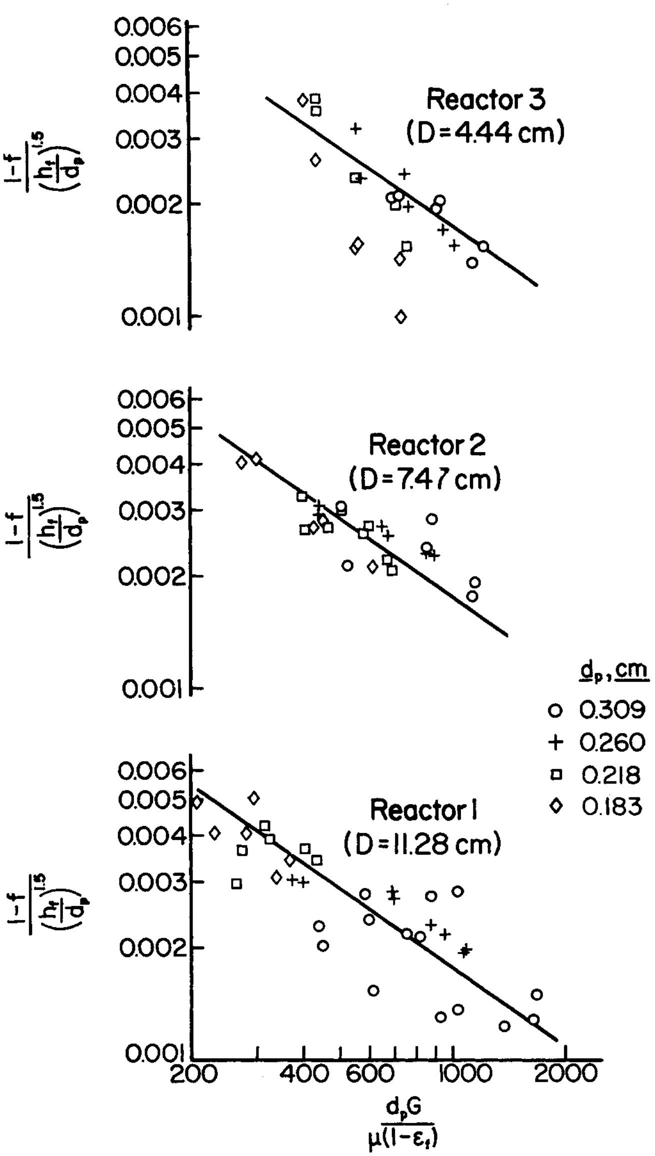

Fig. 4. Relationships between $(1-f)/(H_f/d_p)^{1.5}$ and $d_pG/\mu(1-\epsilon_f)$ for all particle sized and Reactors 1, 2, and 3.

log-mean driving forces have been related as follows:

$$(\Delta y)_a = f(\Delta y)_l \tag{2}$$

where $(\Delta y)_a$ represents the actual integrated mole fraction difference of n-decane and $(\Delta y)_l$ the corresponding log-mean value. Actual values of the factor f are presented in Tables 1, 2, and 3 for the 83 runs of this study. The values of f determined vary from 0.724 to 0.969. For a particle size f approaches 1.00 as the mass velocity G approaches its minimum value G_m. The driving force factor f has been assumed to depend on d_p the average particle size, h_f the average height of the fluidized bed, G the superficial mass velocity of the air, and ϵ_f the void fraction of the fluidized bed. The void fraction ϵ_f is obtained from the fluidized bed height h_f and the corresponding packed bed height h_p by the use of the relationship $(1-\epsilon_f)/(1-\epsilon_p) = h_p/h_f$.

Dimensional analysis considerations suggest that f should depend on the dimensionless groups h_f/d_p and the Reynolds number $d_pG/\mu(1-\epsilon_f)$. The viscosity of air is essentially constant for the conditions of this study. At constant Reynold number, the quantity $1-f$ was found to vary with $(h_f/d_p)^{1.5}$ from the data for each reactor. A plot of $(1-f)/(h_f/d_p)^{1.5}$ against the modified Reynolds number $d_pG/\mu(1-\epsilon_f)$ produced the relationships presented in Figure 4. These relationships can be represented as follows:

$$1 - f = 0.22 \frac{\left(\frac{h_f}{d_p}\right)^{1.5}}{\left[\frac{d_pG}{\mu(1-\epsilon_f)}\right]^{0.70}} \tag{3}$$

Equation (3) represents the behavior of all the data for the three reactors with the exception of four runs with with the smallest particles in the smallest reactor. The calculated values of f and % deviations between the measured values and those calculated with Equation (3) for each run are presented in Tables 1, 2, and 3. For all 83 runs the overall average deviation is 2.45%. For the four runs with the smallest particles the average deviation is 14.4%. For the four runs for the smallest particles in Reactor 3, the following empirical relationship has been found to give improved results over Equation (3):

$$1 - f = 17.90 \times 10^{-5} e^{1.695/d_p^{4/3}} \frac{h_f^{2.00}}{\left[\frac{d_pG}{\mu(1-\epsilon_f)}\right]^{0.0645/d_p^2}} \tag{4}$$

where d_p and h_f are expressed in centimeters. The average deviation for the four runs is 2.96% for Equation (4). For the other runs, the results for Equation (4) are comparable to those obtained with Equation (3). The applicability of these relationships beyond the conditions studied in this investigation requires further verification. A limitation of the approach of this study is that the bed height h_f cannot be so deep that saturation occurs and the log-mean driving force value $(\Delta y)_l$ loses its meaning.

The results of this study indicate that the ratio of the actual driving force to the log-mean driving force f for mass transfer in fluidized beds can be established from measurable parameters of the system. It is reasonable to expect that this concept should also be useful for the analysis of heat transfer in fluidized beds.

ACKNOWLEDGMENT

The authors wish to express their gratitude to the Esso Education Foundation for the fellowship that made this study possible.

NOTATION

d_p = particle size, cm
f = driving force factor, $(\Delta y)_a/\Delta y)_l$
G = superficial mass velocity, g/s cm^2
G_m = minimum superficial mass velocity, g/s cm^2
h_f = height of fluidized bed, cm
h_p = height of packed bed, cm
N_{Re} = modified Reynolds number, $d_pG/\mu(1-\epsilon_f)$
p = vapor pressure of n-decane, mm Hg.
T = absolute temperature, °K
y = concentration of n-decane in air, mole fraction

Greek Letters

Δ = difference
ϵ_f = void fraction of fluidized bed
ϵ_p = void fraction of packed bed
μ = absolute viscosity, g/s cm

Subscripts

a = actual
l = log-mean

LITERATURE CITED

1. Chu, J. C., J. Kalil, and W. A. Wetteroth, "Mass Transfer in a Fluidized Bed," *Chem. Eng. Progr.*, 49, 141 (1953).
2. Sen Gupta, Ashis, and George Thodos, "Mass and Heat Transfer Through Fixed and Fluidized Beds," *ibid.*, 58, 58 (1962).
3. Wilkins, G. S., and George Thodos, "Mass Transfer Driving Forces in Packed and Fluidized Beds," *AIChE J.*, 15, 47 (1969).
4. Zabrodsky, S. S., "Heat Transfer Between Solid Particles and a Gas in a Non-Uniformly Aggregated Fluidized Bed," *Intern. J. Heat Mass Transfer*, 6, 23 (1963).

Manuscript received July 20, 1971; revision received and accepted January 3, 1973.

Restricted Diffusion in Liquids within Fine Pores

The effect on the liquid-phase effective diffusivity in fine pores of the ratio of solute molecular diameter to pore diameter and of preferential solute adsorption was studied by measurements on homogeneous silica-alumina bead catalyst (pore diameter = 3.2 nm). A proposed empirical correlation is based on the investigation of a variety of binary systems of paraffins and aromatic hydrocarbons and of aqueous solutions of sugars.

CHARLES N. SATTERFIELD
CLARK K. COLTON
and
WAYNE H. PITCHER, JR.

Department of Chemical Engineering
Massachusetts Institute of Technology
Cambridge, Massachusetts 02139

SCOPE

The rate of solute diffusion in liquids within finely porous materials becomes observably less than would be expected when the solute molecular size becomes significant with respect to the pore size. Quantitative prediction of the corresponding effective diffusivity can be of importance in guiding experimental work and improving engineering design in such disparate applications as molecular sieve operations, catalytic processing of heavy liquid petroleum fractions, conversion of high molecular weight substrates by immobilized enzymes, gel permeation chromatography, and permeation through natural and synthetic membranes.

Previous work with well-characterized, rigid porous materials include studies with zeolites (Satterfield and Katzer, 1971; Satterfield and Cheng, 1972; Moore and Katzer, 1972) where the pore diameter is of the order of one nm (10Å) and studies with membranes (Beck and Schultz, 1972) with pore diameters of the order of 10 nm (100Å) and greater. The present study examined quantitatively some of the effects of molecular size and physiochemical properties on diffusion in homogeneous silica-alumina catalyst beads having a median pore diameter of 3.2 nm. Effective diffusion coefficients were evaluated by use of transient diffusion measurements, and solute partition and adsorption phenomena were evaluated from equilibrium data. Measurements were made with a large number and variety of binary systems of paraffinic and aromatic hydrocarbons and with aqueous solutions of salts and sugars. The ratio of solute critical molecular diameter (that of the smallest cylinder through which the molecule can pass without distortion) to pore diameter was varied from 0.088 to 0.506.

CONCLUSIONS AND SIGNIFICANCE

The ratio of solute concentration inside pores to concentration outside pores at equilibrium was found to be approximately unity for solutions of saturated hydrocarbons in one another and aqueous solutions of salts and sugars, even when the solute molecules had critical diameters as much as one-half the diameter of the pores. These results are in contrast to theoretical predictions and to previous experimental results obtained with solutions of macromolecules, and they imply the absence of a geometric exclusion effect in the present study. Aromatic hydrocarbons preferentially adsorbed from solution in saturated hydrocarbons, and the magnitude of this effect increased as the number of aromatic rings in the molecule increased.

With nonadsorbing solutes, the logarithm of the ratio of effective to bulk diffusivity decreased linearly with increasing ratio of solute critical molecular diameter to pore diameter, thereby leading to a simple empirical correlation. This behavior does not conform to the prevailing hydrodynamic model for the increased drag on a molecule diffusing in a fine cylindrical pore (Bean, 1972; Beck and Schultz, 1972).

Adsorption further decreased the effective diffusivity below that for an equivalent-sized nonadsorbing solute. An approximate model consistent with the observed data is proposed to describe diffusion occurring in the bulk of the pore and simultaneously in the immediate vicinity of the pore wall with a greatly decreased translation mobility.

Correspondence concerning this paper should be addressed to C. N. Satterfield. W. H. Pitcher is with the Corning Glass Works, Technical Staffs Division, Corning, New York.